

Supplementary Information

Synergistic effect of nanocarbon sphere sheathed on binderless CoMoO₄ electrode for high-performance asymmetric supercapacitor

Roshan Mangal Bhattacharai^a, Sudhakaran Moopri Singer Pandiyarajan^a, Shirjana Saud^a, Sang Jae Kim^b, Young Sun Mok^{a*}

^a Department of Chemical and Biological Engineering, Jeju National University, Jeju-63243,
Republic of Korea.

^b Nanomaterials and System Laboratory, Department of Mechatronics Engineering, Jeju National
University, Jeju 63243, Republic of Korea.

*Corresponding author: smokie@jejunu.ac.kr

Tel.: +82-064-754-3682; Fax: +82-64-755-367

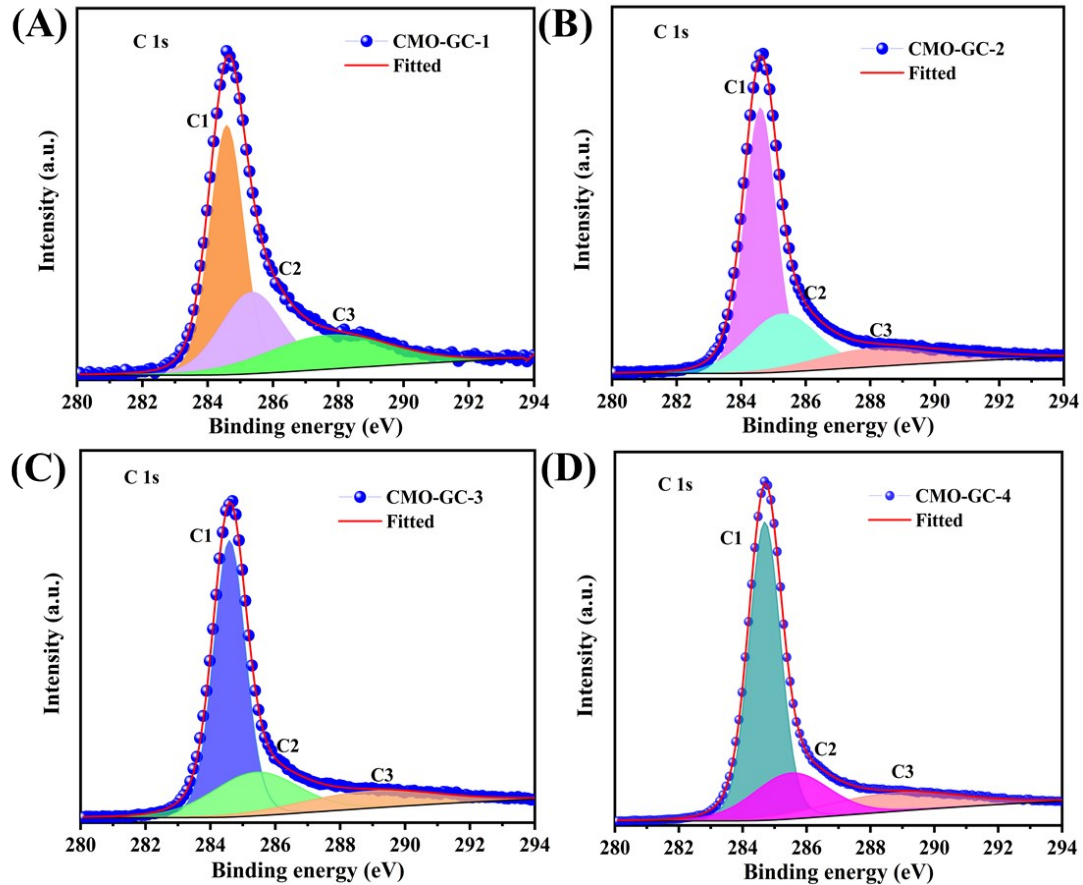


Figure S1. XPS core level profile of C 1s of the CMO-GC-1 (A), CMO-GC-2 (B), CMO-GC-3 (A), and CMO-GC-4 (D).

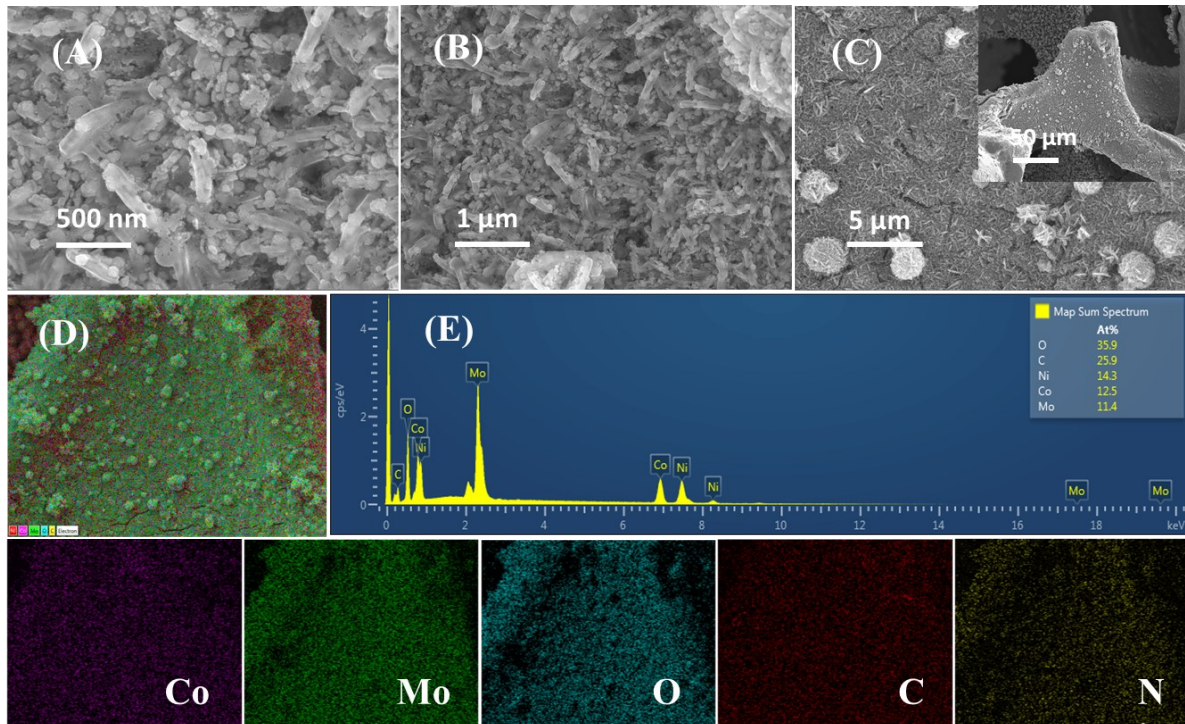


Figure S2. Field emission-scanning electron (FE-SEM) micrographs of as prepared CMO-GC-1 electrode (A-C) at different magnification, inset at 50 μm magnification; FE-SEM micrographs for elemental mapping of different elements of CMO-GC-1 (D), (i) cobalt, (ii) molybdenum, (iii) oxygen, (iv) carbon, and (iv) nickel; SEM- EDS elemental spectrum of CMO-GC-1 electrode (E).

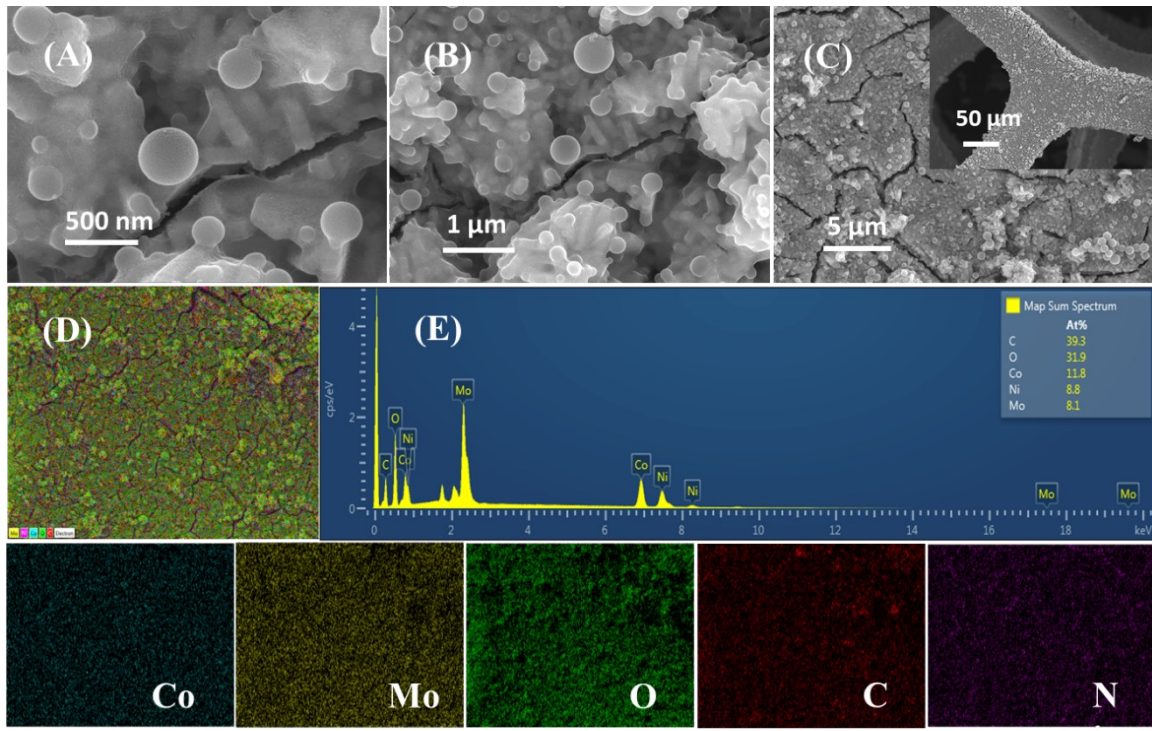


Figure S3. FE-SEM images of as prepared CMO-GC-3 electrode (A-C) at different magnification, inset at 50 μm magnification; FE-SEM micrographs for elemental mapping of different elements of CMO-GC-3 (D), (i) cobalt, (ii) molybdenum, (iii) oxygen, (iv) carbon, and (iv) nickel; SEM-EDS elemental spectrum of CMO-GC-3 electrode (E).

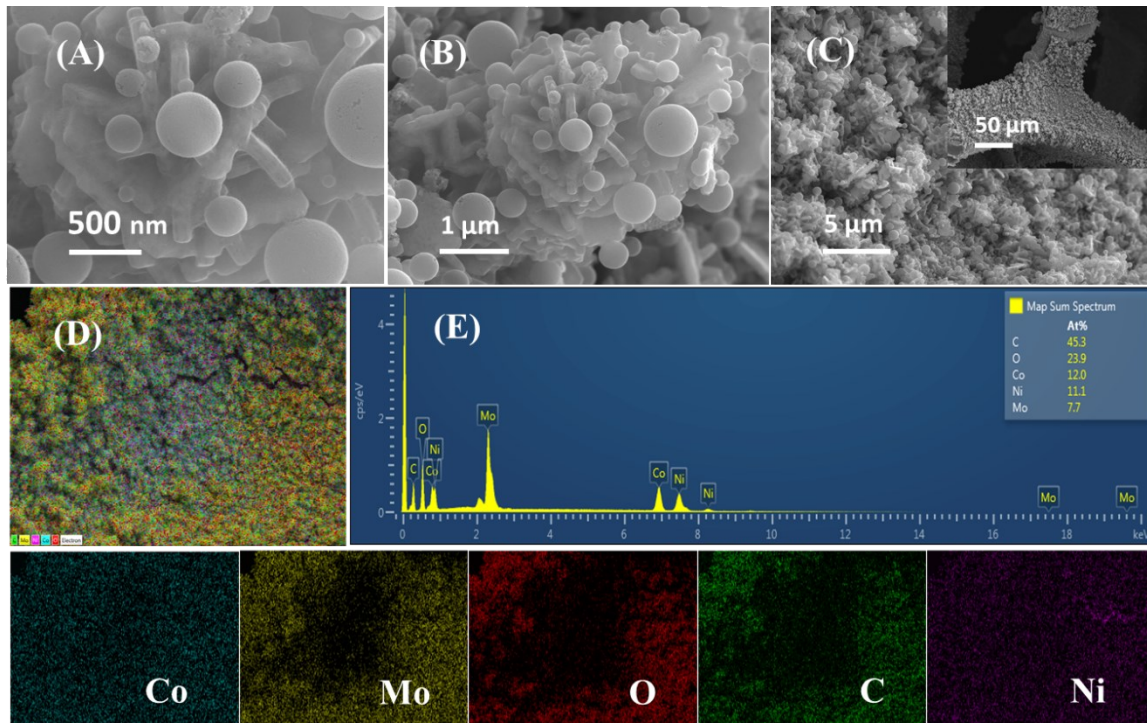


Figure S4. FE-SEM images of as prepared CMO-GC-4 electrode (A-C) at different magnification, inset at 50 μm magnification; FE-SEM micrographs for elemental mapping of different elements of CMO-GC-4 (D), (i) cobalt, (ii) molybdenum, (iii) oxygen, (iv) carbon, and (iv) nickel; SEM-EDS elemental spectrum of CMO-GC-4 electrode (E).

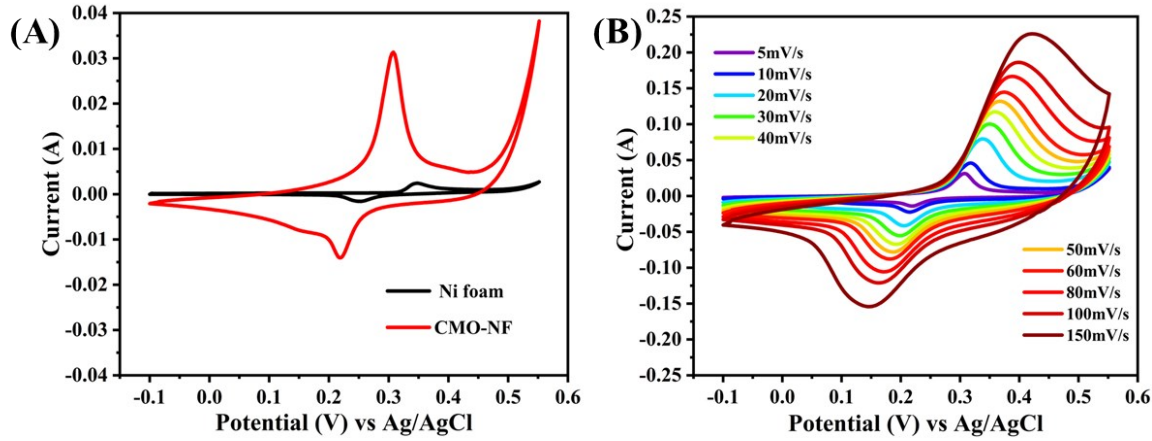


Figure S5. Electrochemical performance of as prepared pristine nickel foam and CMO-NF electrode in three electrode system. Comparative cyclic voltammetry profile of nickel foam and CMO-NF electrode measured at constant scan rate of 5 mV/s (A), and cyclic voltammetry profile of the CMO-NF electrode at various scan rates (5 to 150 mV/s) (B).

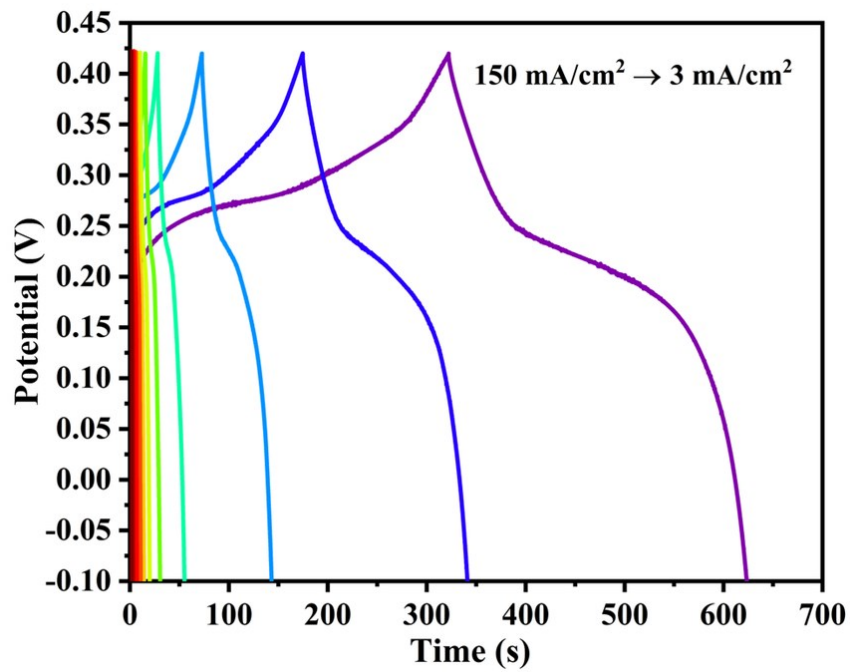


Figure S6. Galvanostatic charge-discharge profile of CMO-NF electrode measured at different current (3 mA – 150 mA).

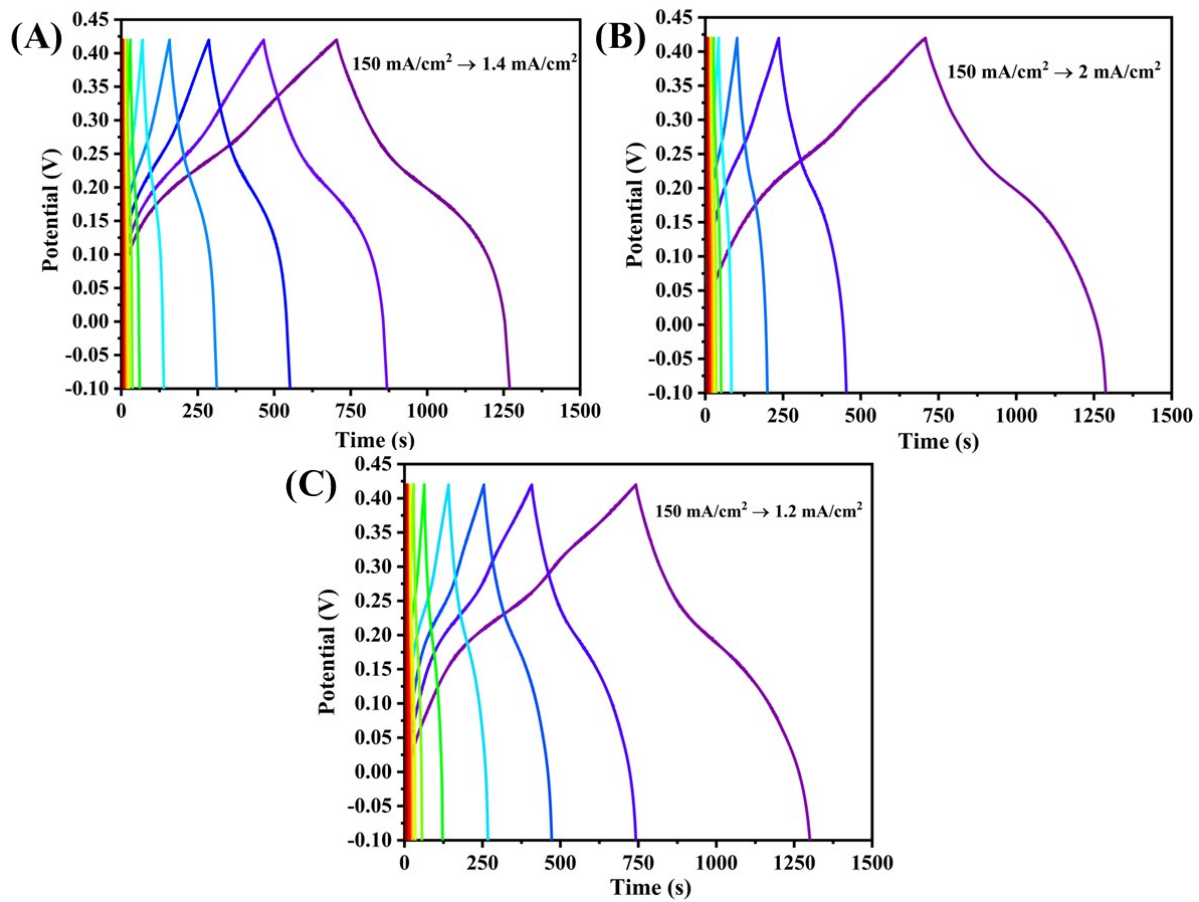


Figure S7. Galvanostatic charge-discharge profile of as prepared CMO-GCs electrode measured at different current ($1\text{mA} - 150\text{ mA}$); GCD of CMO-GC-1 electrode (A), GCD of CMO-GC-3 electrode (B), and GCD of CMO-GC-4 electrode (C).

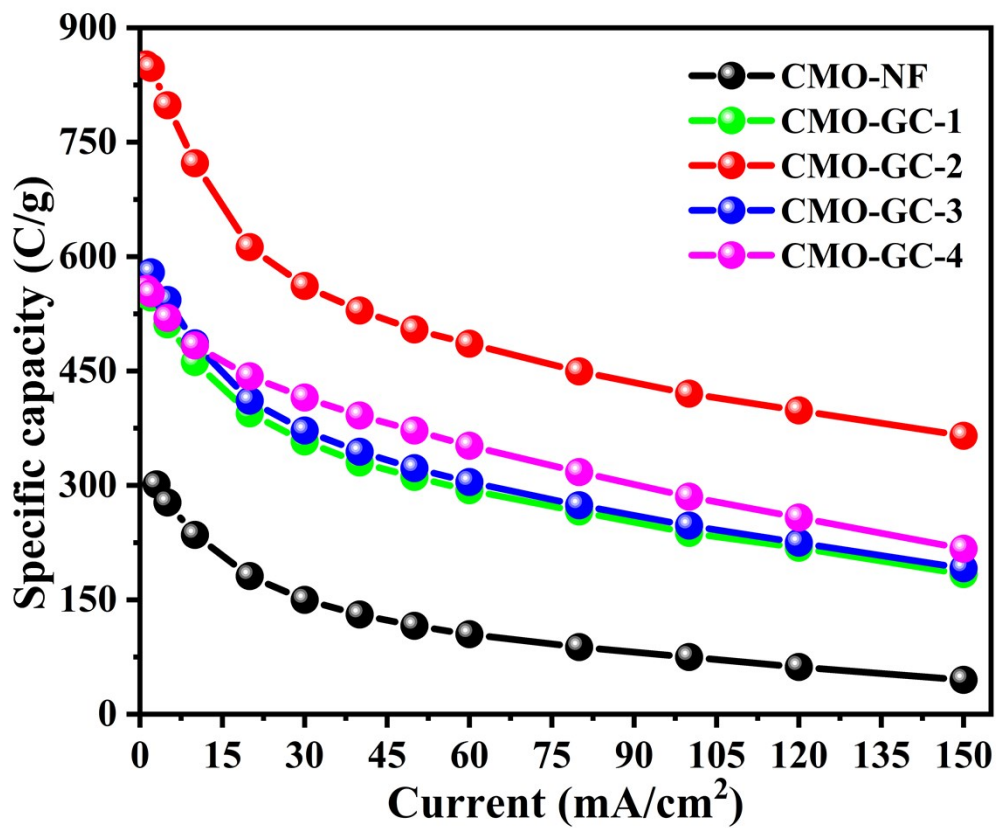


Figure S8. Effect of current densities on specific capacitance measured from GCD profile of as prepared CMO-GCs electrode by three electrodes system.

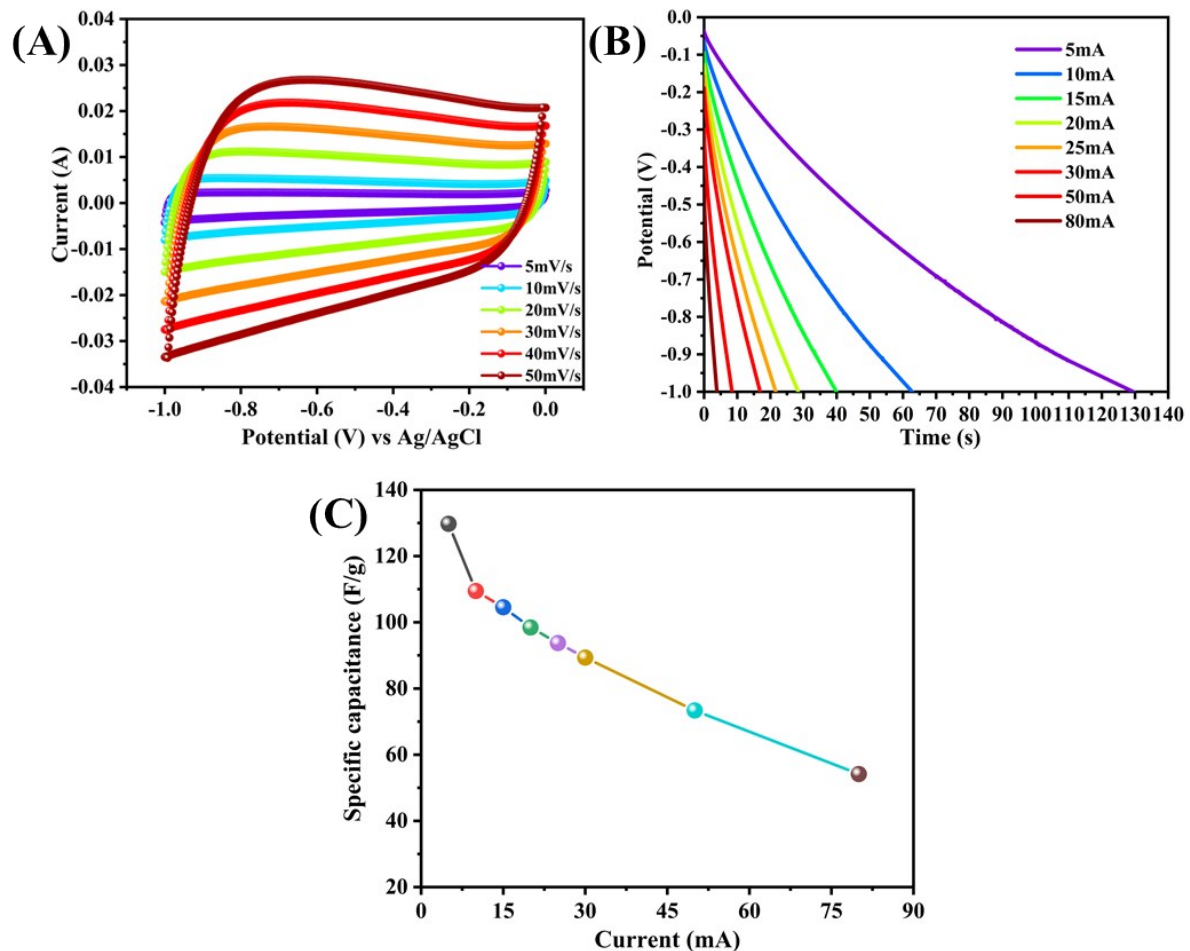


Figure S9. Electrochemical performance of as-prepared activated carbon in three-electrode system. cyclic voltammetry profile of activated carbon electrode measured at various scan rates (5 to 50 mV/s) (A), and Galvanostatic charge-discharge curves at different current densities (5 to 80 mA/cm²) (B), and effect of current on the specific capacitance of AC electrode (C).

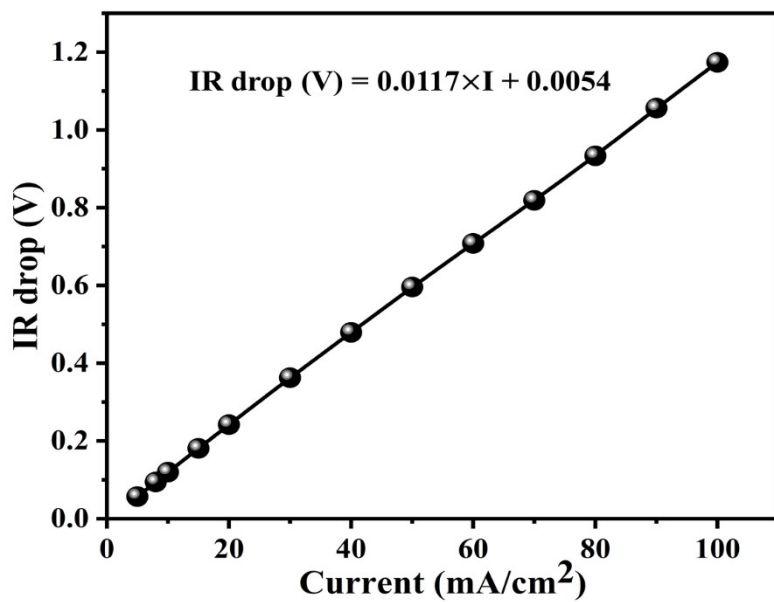


Figure S10. Potential drop associated with CMO-GC/AC asymmetric supercapacitor internal resistance (IR loss) vs. different discharge current densities.

Table S1. The electrochemical metrics of CMO-GC-2 electrode with reported CoMoO₄ based binder-free electrodes in the three-electrode system.

S. No.	Electrode configuration	Potential window (V)	Current density	Specific capacitance	Electrolyte	Ref
1.	CoMoO ₄ / MWCNTs	0.8 V	1 A/g	76.8 C/g (96 F/g)	1 M KOH	¹
2.	CoMoO ₄ • 0.75H ₂ O/PANI	0.6 V	1 A/g	228 C/g (380 F/g)	1 M Na ₂ SO ₄	²
3.	CoMoO ₄ @Carbon cloth	0.5 V	2 A/g	226 C/g (452 F/g)	1 M KOH	³
4.	CoMoO ₄ • 0.9H ₂ O– rGO	0.45 V	1 A/g	360.99 C/g (802.2 F/g)	1 M KOH	⁴
5.	NiO@CoMoO ₄	0.4 V	0.5 A/g	339.2 C/g (848 F/g)	2 M KOH	⁵
6.	CoMoO ₄ @RGO	0.5 V	1 A/g	428.1 C/g (856.2 F/g)	2 M KOH	⁶
7.	CoMoO ₄ –NiMoO ₄ • x H ₂ O	0.4 V	2.5 mA/cm ²	415.6 C/g (1039 F/g)	2 M KOH	⁷
8.	Co ₃ O ₄ @CoMoO ₄ core/shell	0.6 V	1 A/g	624 C/g (1040 F/g)	3 M KOH	⁸
9.	CoMoO ₄ /C	0.5 V	1 A/g	225.8 C/g (451.6 F/g)	3 M KOH	⁹
10.	CMO-GC	0.52 V	1 A/g	851.85 C/g (1638.17 F/g)	2 M KOH	This paper

Table S2. Performance metrics of CMO-GC-2//AC (ASC) device with reported multicomponent nano shaped electrode of ASC device.

S. No.	ASC device	Potential window (V)	Energy density (Wh/kg)	Power density (W/kg)	Electrolyte	Ref
1	CoMoO ₄ -HMPA/NF//AC	1.6	0.321 mWh/c m ²	1.7 mW/cm	3 M KOH	¹⁰
2.	NiCo ₂ O ₄ NG@CF	1.65	6.6	425	PVA/KOH gel	¹¹
3.	NiCoMoCuO	1.6	13.9	340.4	1 M KOH	¹²
4.	CoMoO ₄ -3D Graphene//AC	1.8	21.1	300	2 M KOH	¹³
5.	NiCo ₂ O ₄ @Mn MoO ₄ CSNAs//AC	1.6	15.0	336	3 M KOH	¹⁴
6.	ZnCo ₂ O ₄ /H: ZnO NRs//AC	1.5	3.7	653.3	6 M KOH	¹⁵
7.	CoMoO ₄ -NiMoO ₄ //AC	1.4	16.0	1600	2 M KOH	⁷
8.	α -CoMoO ₄ //AC	1.2	14.5	1000	2 M LiOH	¹⁶
9.	CoMoO ₄ /r-GO	1.5	8.1	187.5	1 M NaOH	¹⁷
10.	NiMoO ₄ /CoMo O ₄	1.5	23.1	375	2 M KOH	¹⁸
11.	CMO-GC//AC	1.5	36.8	152.8	2 M KOH	This work

Table S3. The electrochemical impedance spectroscopy results of CMO-GC-2//AC device.

	R _s (Ω)	R _{ct} (Ω)	Z _w (mMho)	CPE (mMho)	C (F)
Before 5000 cycles	3.25	7.2	9	0.9	1.4
After 5000 cycles	2.10	8.0	100	3.0	1.3

References

- 1 Z. Xu, Z. Li, X. Tan, C. M. B. Holt, L. Zhang, B. S. Amirkhiz and D. Mitlin, *RSC Adv.*, 2012, **2**, 2753–2755.
- 2 M. Mandal, D. Ghosh, S. Giri, I. Shakir and C. K. Das, *RSC Adv.*, 2014, **4**, 30832–30839.
- 3 G. Xu, X. Ren, Z. Zhang, H. Zhang, X. Sun, X. Qi, P. Wan and Z. Huang, *Nanoscale*, 2016, **8**, 13273–13279.
- 4 K. Xu, J. Chao, W. Li, Q. Liu, Z. Wang, X. Liu, R. Zou and J. Hu, *RSC Adv.*, 2014, **4**, 34307–34314.
- 5 X. J. Ma, L. Bin Kong, W. Bin Zhang, M. C. Liu, Y. C. Luo and L. Kang, *RSC Adv.*, 2014, **4**, 17884–17890.
- 6 L. Jinlong, Y. Meng, K. Suzuki and H. Miura, *Microporous Mesoporous Mater.*, 2017, **242**, 264–270.
- 7 M. C. Liu, L. Bin Kong, C. Lu, X. J. Ma, X. M. Li, Y. C. Luo and L. Kang, *J. Mater. Chem. A*, 2013, **1**, 1380–1387.
- 8 Z. Gu, R. Wang, H. Nan, B. Geng and X. Zhang, *J. Mater. Chem. A*, 2015, **3**, 14578–14584.
- 9 N. Padmanathan, K. M. Razeeb and S. Selladurai, *Ionics (Kiel)*., 2014, **20**, 1323–1334.
- 10 Q. Li, Y. Li, J. Zhao, S. Zhao, J. Zhou, C. Chen, K. Tao, R. Liu and L. Han, *J. Power Sources*, 2019, **430**, 51–59.
- 11 S. T. Senthilkumar, N. Fu, Y. Liu, Y. Wang, L. Zhou and H. Huang, *Electrochim. Acta*, 2016, **211**, 411–419.
- 12 T.-Y. Chen and L.-Y. Lin, *Electrochim. Acta*, 2019, **298**, 745–755.
- 13 X. Yu, B. Lu and Z. Xu, *Adv. Mater.*, 2014, **26**, 1044–1051.
- 14 Y. Yuan, W. Wang, J. Yang, H. Tang, Z. Ye, Y. Zeng and J. Lu, *Langmuir*, 2017, **33**, 10446–10454.
- 15 B. Deka Boruah, A. Maji and A. Misra, *Nanoscale*, 2017, **9**, 9411–9420.
- 16 S. Baskar, D. Meyrick, K. S. Ramakrishnan and M. Minakshi, *Chem. Eng. J.*, 2014, **253**, 502–507.
- 17 G. K. Veerasubramani, K. Krishnamoorthy and S. J. Kim, *RSC Adv.*, 2015, **5**, 16319–16327.
- 18 P. Zhang, X. Zhang and G. Li, *Ionics (Kiel)*., 2020, **26**, 393–401.